Performance-Based Design in Earthquake Geotechnical Engineering – Kokusho, Tsukamoto & Yoshimine (eds)
© 2009 Taylor & Francis Group, London, ISBN 978-0-415-55614-9

New Biot's equation for finite element analysis

N. Yoshida
Tohoku Gakuin University, Japan

Y. Ohya & T. Sugano
Port and Airport Research Institute, Japan

ABSTRACT: A finite element modeling for liquefaction analysis, which is free from volume locking and hourglass instability is proposed. Volume locking occurs under undrained condition or similar in the liquefaction analysis, and hourglass instability occurs when excess reduced integration is employed to avoid volume locking. Proposed method employs different numerical integration schemes for porewater and soil skeleton to build element matrices: ordinary integration for soil skeleton and reduced integration for all other element matrices. Numerical examples are made to evaluate effectiveness and accuracy of the proposed method by comparing other existing methods. The proposed method is shown to be accurate and to be free from both volume locking and hourglass instability. Finally, case study of liquefied ground is made to simulate Akita port damaged during the 1983 Nihonkai-chubu earthquake, and succeeded to explain the damage.

1 INTRODUCTION

Many design specifications have employed concept of performance-based design after the 1995 Hyogoken-nambu (Kobe) earthquake in Japan. Liquefaction analysis is sufficient to predict onset of soil liquefaction in many past design specifications, because remedial measures are considered if liquefaction will occur. It is not enough, however, in the performance based design because onset of liquefaction is allowed to occur if expected functions of a structure are not lost. It indicates that prediction of the behavior after the soil liquefaction is required with high accuracy. Past blind tests and bench mark calculation have shown, however, that there exists many scattering in the existing computer programs (see Yoshida, 1998, for example), and that evaluated displacement especially scatters widely (e.g., JSCE, 2003).

Two issues are at least to be considered in predicting displacement after the soil liquefaction. The one is a stress-strain model. Since state point comes very close to failure line during liquefaction, slight difference of stress by the analysis will result in large difference of strains and displacements. The other is a finite element formulation discussed in this paper.

Volume change of porewater is expected to be very small in the liquefied soil during earthquakes because porewater that flowed into or out of the soil elements is very small as duration of earthquakes are very short. A typical example is an undrained condition that has frequently employed in the past liquefaction analyses. Under the undrained condition, porewater does not flow out of and flow in an element, or soil skeleton behaves with porewater as one body, which will be called as apparent soil element in this paper. Since bulk modulus of water is much larger than that of soil skeleton, Poisson's ratio of the apparent soil element is close to 0.5, or volume change hardly occurs.

Volume locking occurs if Poisson's ratio is close to 0.5 as pointed out by Yasuda et al. (1999) and Yamada (2007), et al. It occurs because apparent stiffness of finite element becomes very large, resulting in very small displacement (see Yasuda et al., 1999, for example, to grasp how it works). In the case of a quadrilateral element under no volume change condition, for example, deformation into trapezoid shape, in which there is no volume change in a whole element, requires significant volume change in each integration point to evaluate element stiffness matrix, but volume change is prohibited by the constitutive model, which result in very stiff element stiffness both for shear and volume change. It hardly occurs in the ordinary geotechnical problems, but it occurs in the liquefaction analysis because volume change is not allowed in apparent soil element although it is possible in only soil skeleton.

Several methods have been proposed to avoid volume locking. Reduced Integration is the most popular solution, in which reduced integration is made to develop element stiffness matrix. Volume locking does not occur if integration is made by means of the Gauss-Legendre integration scheme by using quantities at the center of a quadrilateral element where volume change does not occur under a trapezoid shape deformation. Some computer programs such as LIQCA (LIQCA dev. Team, 2002) employed this method. Use

of excess reduced integration such as this, however, creates another problem which is usually called hourglass instability or zero-energy mode deformation. Since volumetric strain is zero at the integration point in the preceding case, a trapezoid shape deformation is free to occur under zero energy, which is the reason why it is called zero-energy mode. On the other hand, the name of hourglass instability comes from its shape; appearance of two deformed neighboring elements looks like an hourglass.

Anti-hourglass stiffness has been proposed to avoid hourglass instability, and some FE computer programs employ it (Yoshida, 1993; Fukutake, 1997). Concept to add specially designed stiffness was proposed against shear locking (Flanagan, 1981) related to the problem of beam bending. Various improvements have been proposed on shear locking after that. Selective Reduced Integration (SRI) method (Bathe, 1982), for example, is one of the successful methods in this field, in which deformation is separated into shear and volume change and excess reduced integration is made only for shear deformation. Few researches were, however, made on volume locking, partly because there is few materials that show no-volume change behavior, except mixture such as soil particle and water treated in this paper. Although phenomena are similar between shear locking and volume locking, mechanisms are different. In this paper, we propose a method to avoid volume locking, and examine accuracy of the proposed method through numerical example.

2 PROPOSED METHOD

In the liquefaction analysis, apparent Poisson's ration comes close to 0.5. In the undrained condition, which is frequently employed in the liquefaction analysis because porewater that goes out of or comes in an soil element is very small, apparent bulk modulus (bulk modulus of the mixture of soil particle and porewater), yields $K + K_w/n$, where K is bulk modulus of soil skeleton, K_w is that of water, and n is porosity. Since K_w is much larger than K, Poisson's ratio is large even at the state before earthquakes; it is usually 0.45 or larger. It becomes larger as shear modulus becomes smaller because of generation of excess porewater pressure or decease of effective confining stress.

Poisson's ratio of soil skeleton is not so large; it is about 0.3 (Kokusho, 1980). The large Poisson's ratio, therefore, comes as soil particles and porewater behave as one body. Partly because formulation becomes much simpler when soil is treated as such a way, past improvement on this problem is made only on undrained condition; governing equation becomes identical with that of total stress analysis by replacing bulk modulus into that of mixture, $K + K_w/n$. One of the author apply anti-hourglass stiffness only on soil skeleton (Yoshida, 1993), and succeeded to consider drainage between soil elements as well as undrained condition. According to this experience, however, use of specially defined additional stiffness (anti-hourglass stiffness) is inconvenient in practical use, and a more convenient method is required.

Finite element formulations of Biot's equation (Biot, 1941) which deals with two phase material have been proposed by many researchers (see JGS, 2007, for past formulations, for example). These formulations, however, does not tell how to solve the problem discussed in this paper; most of them do not deal with detailed numerical integration scheme required to solve volume locking.

2.1 *Governing equations*

We start our governing equations from u-U formulation, the most accurate formulation of Biot's equation. The overall equilibrium equation is

$$\mathbf{L}^{\mathbf{T}}\sigma - \rho\mathbf{b} + (\rho - n\gamma_f)\ddot{\mathbf{u}} + n\rho_f\ddot{\mathbf{U}} = 0 \tag{1}$$

It is noted that descriptions are made by, so-called, Voigt form, and bold letters denote matrix or vector. The variable $\mathbf{u}$ denotes displacement of soil skeleton, $\mathbf{U}$ is that of porewater, $\boldsymbol{\rho}$ is density of soil (mixture of soil particle and water), $\mathbf{b}$ is body force, ρ_f is density of water, and $\boldsymbol{\sigma}$ is total stresses. The differential operator $\mathbf{L}$ is introduced in calculating strain from displacement in two-dimensional analysis as

$$\mathbf{L}^T = \begin{bmatrix} \partial/\partial x & 0 & \partial/\partial y \\ 0 & \partial/\partial y & \partial/\partial x \end{bmatrix} \tag{2}$$

Next, equilibrium equation of only porewater is given by

$$\nabla p + \rho_f \mathbf{k}^{-1}(\dot{\mathbf{U}} - \dot{\mathbf{u}}) + \rho_f \frac{n-1}{n}\ddot{\mathbf{u}} + \frac{\rho_f}{n}\ddot{\mathbf{U}} - \rho_f \mathbf{b} \tag{3}$$

where p is excess porewater pressure, g is acceleration of gravity, k is permeability, n is porosity, and $\nabla = \{\partial/\partial x \quad \partial/\partial y\}$ is differential operator. Finally, continuity equation yields

$$\mathbf{m}^{\mathrm{T}}\dot{\boldsymbol{\varepsilon}} = n\nabla^{\mathrm{T}}(\dot{\mathbf{U}} - \dot{\mathbf{u}}) + \frac{n}{K_w}\dot{p} \tag{4}$$

where $\mathbf{m}$ is a vector that works same with Kronecker's δ in the tensor expression; argument of $\mathbf{m}$ is unity for normal component and is zero for shear component. Excess porewater pressure p can be eliminated from Equations (3) and (4) under the assumption that K_w is not infinite, resulting in u-U formulation. The bulk modulus of water K_w is usually assumed to be infinite in the consolidation analysis. Infinite K_w, however, result in infinite P-wave velocity in the dynamic

problem, therefore, it is hardly used. This indicates that u-U formulation is also an exact formulation of Biot's equation. These equations are resulted into a finite element form as (see JGS (2007) for detailed derivation)

$$\begin{bmatrix} \mathbf{M}^u & \mathbf{0} \\ \mathbf{0} & \mathbf{M}^U \end{bmatrix} \begin{Bmatrix} \ddot{\overline{\mathbf{u}}} \\ \ddot{\overline{\mathbf{U}}} \end{Bmatrix} + \begin{bmatrix} \mathbf{C}^{uu} & -\mathbf{C}^{uU} \\ -\mathbf{C}^{uUT} & \mathbf{C}^{UU}{}_S \end{bmatrix} \begin{Bmatrix} \dot{\overline{\mathbf{u}}} \\ \dot{\overline{\mathbf{U}}} \end{Bmatrix} + \begin{bmatrix} \mathbf{K}+\mathbf{K}^{uu} & \mathbf{K}^{uU} \\ \mathbf{K}^{uU\mathrm{T}} & \mathbf{K}^{UU} \end{bmatrix} \begin{Bmatrix} \overline{\mathbf{u}} \\ \overline{\mathbf{U}} \end{Bmatrix} = \begin{Bmatrix} \mathbf{F}^u \\ \mathbf{F}^U \end{Bmatrix} \tag{5}$$

where variable with upper bar indicates quantity that belongs to a node. Displacement in an element can be obtained by using displacement at all nodes and interpolation function $\mathbf{N}^u$ and $\mathbf{N}^U$ as

$$\mathbf{u} = \mathbf{N}^u \overline{\mathbf{u}}, \quad \mathbf{U} = \mathbf{N}^U \overline{\mathbf{U}} \tag{6}$$

where

$$\mathbf{M}^u = \int_V (\mathbf{N}^u)^{\mathrm{T}} (\rho - n\rho_f) \mathbf{N}^u dV : \text{ density of soil skeleton}$$

$$\mathbf{M}^U = \int_V \mathbf{N}^{U\mathrm{T}} n\rho_f \mathbf{N}^U dV : \text{ density of porewater}$$

$$\mathbf{C}^{uu} = \int_V \mathbf{N}^{u\mathrm{T}} \rho_f g \mathbf{k}^{-1} n^2 \mathbf{N}^u dV : \text{ influence of viscosity on soil skeleton}$$

$$\mathbf{C}^{uU} = \int_V \mathbf{N}^{u\mathrm{T}} \rho_f g \mathbf{k}^{-1} n^2 \mathbf{N}^U dV : \text{ interaction of viscosity}$$

$$\mathbf{C}^{UU} = \int_V \mathbf{N}^{U\mathrm{T}} \rho_f g \mathbf{k}^{-1} n^2 \mathbf{N}^U dV : \text{ influence of viscosity on porewater}$$

$$\mathbf{K} = \int_V (\mathbf{L}\mathbf{N}^u)^{\mathrm{T}} \mathbf{D} (\mathbf{L}\mathbf{N}^u) dV : \text{ element stiffness of soil skeleton}$$

$$\mathbf{K}^{uu} = \int_V (\nabla^{\mathrm{T}} \mathbf{N}^u)^{\mathrm{T}} \frac{(1-n)^2}{n} K_w (\nabla^{\mathrm{T}} \mathbf{N}^u) dV : \text{ interaction of stiffness}$$

$$\mathbf{K}^{uU} = \int_V (\nabla^{\mathrm{T}} \mathbf{N}^u)^T (1-n) K_w (\nabla^{\mathrm{T}} \mathbf{N}^U) dV : \text{ interaction of stiffness}$$

$$\mathbf{K}^{UU} = \int_V (\nabla^{\mathrm{T}} \mathbf{N}^U)^T n K_w (\nabla^{\mathrm{T}} \mathbf{N}^U) dV : \text{ element stiffness of porewater}$$

$$\mathbf{F}^u = \int_V \mathbf{N}^{u\mathrm{T}} (\rho - n\rho_f) \mathbf{b} dV + \int_S \mathbf{N}^{u\mathrm{T}} \mathbf{T}^u dS + \int_V \mathbf{N}^{u\mathrm{T}} (1-n) \mathbf{T}^p dS : \text{ external force on soil skeleton}$$

$$\mathbf{F}^U = \int_S \mathbf{N}^{U\mathrm{T}} n \mathbf{T}^p dS + \int_V \mathbf{N}^{U\mathrm{T}} n\rho_f \mathbf{b} dV : \text{ external force on porewater}$$

$$\mathbf{T}^u = -\mathbf{s}\sigma' : \text{ force on a face of soil skeleton}$$

$$\mathbf{T}^p = -\mathbf{t}p : \text{ force on a face of porewater}$$

where $\mathbf{s}$ is a direction cosine matrix, $\mathbf{t}$ is a direction cosine vector of the surface load, σ' is effective stress vector and $\mathbf{D}$ is stiffness matrix of soil skeleton. Integrals dV and dS indicate integral in an entire.

2.2 *Integration scheme in element*

In the formulation of Biot's equation, it is natural to model soil skeleton and porewater separately, and to consider interaction between them in the FE modeling. Integrations in an element are calculated by the Gauss-Legendre integration. Stiffness matrix K, for example, is calculated for a quadrilateral isoparametric element in a two-dimensional problem as,

$$\mathbf{K} = \int_V (\mathbf{L}\mathbf{N}^u)^{\mathrm{T}} \mathbf{D} (\mathbf{L}\mathbf{N}^u) dV \approx \sum_{i=1}^{2} \sum_{j=1}^{2} w_{ij} (\mathbf{L}\mathbf{N}^u)_{ij}^T \mathbf{D}_{ij} (\mathbf{L}\mathbf{N}^u)_{ij} \tag{7}$$

where w_{ij} is an weighting coefficient and subscripts i and j indicates integration points. Number of integration points in one direction is two in Equation 7, which is, therefore, called 2 point integration in the following although there is four integration points in an element in the two-dimensional analysis. As explained in the preceding, this integration causes volume locking under no-volume change condition or similar. In order to avoid volume locking, we need to proceed a more excess reduced integration, in which number of integration point is one instead of two, and is usually called one-point integration.

A simple two-dimensional problem is dealt with in this paper, which uses quantities only in two dimensions, and is different from plane strain or plane stress condition. Then the stiffness matrix is divided into shear deformation related term and the rest as

$$D = \begin{bmatrix} 2G & 0 & 0 \\ 0 & 2G & 0 \\ 0 & 0 & G \end{bmatrix} + \begin{bmatrix} K-G & K_G & 0 \\ K-G & K_G & 0 \\ 0 & 0 & 0 \end{bmatrix} \tag{8}$$

SRI against shear locking employs two-point integration to latter part (volume change term) and one-point integration to former part (shear deformation term). Therefore, we need to employ one-point integration to the latter term and two-point integration to the former term in order to avoid volume locking. This method is, however, inconvenient in the liquefaction analysis in which the consideration of dilatancy (volume change associated with shear deformation) is indispensable; constitutive model is not so simple as Equation (8).

Water is originally instable against hourglass deformation because it does not have shear resistance, and Poisson's ratio of soil skeleton is far from no volume change deformation. Therefore, it is reasonable to employ two-point integration for soil skeleton and one-point integration for water. Then a new problem appears; which integration scheme is to be employed in the interaction term such as $\mathbf{K}^{uu}$, $\mathbf{K}^{uU}$, $\mathbf{K}^{UU}$, $\mathbf{C}^{uu}$, $\mathbf{C}^{uU}$, and $\mathbf{C}^{UU}$. As shown in the next section, we suggest using one-point integration for all these integrations; two-point integration is made only for $\mathbf{K}$. It means that deformation like hourglass mode is carried only by soil skeleton, which is natural feature because porewater does not resists against hourglass deformation.

3 NUMERICAL EXAMPLE

Two numerical examples are made to show effectiveness and accuracy of the proposed method. The first example discuss accuracy of method, and the second is an example for liquefaction analysis.

3.1 *Choice of integration*

There appears several element stiffness matrices in the finite element formulation in Equation (5), and numerical integration scheme on each matrix are of our interest. Accuracy of each integration scheme is evaluated in this sub-section by using a simple model.

3.1.1 *Analyzed model*

A simple rectangular element shown in Figure 1 is used to examine accuracy of the finite element modeling scheme. In order to escape from factors that are not related to the present problem, we apply hourglass force of Q (pair of two force couples) which is also shown in Figure 1. Accuracy is examined by comparing hourglass displacement δ (deformation like trapezoid shape shown in Figure 1) under the action of hourglass force Q. Parameters used in the example are also shown in the figure, where G is shear stiffness and ν is Poisson's ratio of soil skeleton. Undrained condition ($u = U$) is also employed in order to make discussion simple, under which apparent Poisson's ratio of an apparent soil element becomes 0.499.

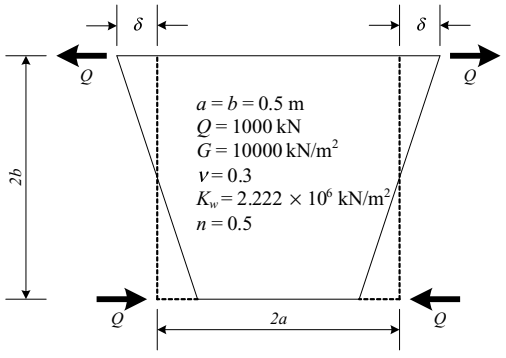

Figure 1. Rectangular model.

3.1.2 *Beam analogy*

Exact solution of the problem in Figure 1 is not known. We employ beam analogy to obtain a solution that can be compared with proposed method, because deformation in Figure 1 looks like deformation of beam under pure bending. If it is pure bending deformation, moment-curvature relationship is obtained based on Bernoulli-Euler theory, as

$$M = EI\kappa \tag{9}$$

where M is bending moment, E is young's modulus, I is moment of inertia, and κ is curvature. Equilibrium condition in Figure 1 is

$$M = 2Qb \tag{10}$$

Then hourglass deformation is calculated as $\delta = b\kappa$, yielding $\delta = 0.2308$ m under the action of $Q = 1000$ kN. It is noted that this is not exact solution because bending deformation and hourglass deformation assumed here are a little different to each other. The width 2a is, for example, infinitesimally small in the beam theory whereas it is finite value in Figure 1, top and bottom edges curves in the beam whereas it is straight, and bending moment is caused by distributed load in the beam whereas it is caused by concentrated force at node. In other words, hourglass deformation in Figure 1 is obtained by restraining the bending deformation. Therefore, expected displacement against hourglass deformation is smaller than the displacement by the beam theory in Equation (9).

3.1.3 *Element stiffness matrix*

Parametric studies are made on the method of analysis and method of integration in an element. Both one phase (total stress) analysis and two phase analysis are made.

In the total stress analysis, soil skeleton and porewater behave as one body in whole element, which is

called an apparent element in the preceding. The integration of element stiffness matrix **K** is of interest in this case. The governing equation is obtained by setting bulk modulus to be $K + K_w/n$. The following 6 integration methods are investigated.

a. *Two-point integration*: Integration at two points.
b. *Reduced Integration*: Integration at one point.
c. *Reduced Integration with anti-hourglass stiffness*: Anti-hourglass stiffness (Flanagan, 1981) is added to the stiffness obtained by one-point integration.
d. *Selective Reduced Integration*: Stiffness matrix is divided into shear deformation component and volume change component, and two-point integration is employed to the shear deformation component and one-point integration to the volume change component.
e. *Selective Reduced Integration only for soil skeleton*: Only soil skeleton is considered, and stiffness matrix is evaluated by SRI method. This case is made only to compare with other methods.
f. *Two-point integration only of soil skeleton*: Same as before except that integration is made by two-point integration.

Next, two phase material is modeled by *u-U* formulation. The constraint of undrained condition is given only at nodes as $U = u$ in this formulation. In this example, however, displacements become same in whole elements because the same interpolation functions are used for both soil skeleton and porewater. The following cases are examined by changing integration schemes.

a. *Two-point integration*: Integration at two points for all matrices.
b. *Reduced Integration*: Integration at one point for all matrices.
c. *Proposed method*: Two-point integration is used only to stiffness matrix of soil skeleton **K** and one-point integration to the rest.
d. *Selective Reduced Integration*: SRI is applied only to stiffness matrix of soil skeleton **K** and one-point integration to the rest.

3.1.4 *Results and discussion*

Results of analysis are summarized in Table 1.

In the total stress analysis, displacement by two-point integration is very small to be order of 1/100, indicating the appearance of volume locking. As stiffness matrix becomes singular in one-point integration because no strain occurs at the center of an element although is not a rigid 1 body deformation, displacement cannot be obtained or infinite displacement is expected in this case, therefore the result is shown as 'infinite' in the table. On the other hand, stable behavior is obtained by introducing anti-hourglass stiffness, and the result is close but a little smaller compared with the beam theory. Volume locking does not occur when SRI is used because effect of volume change is evaluated at the center. In addition, hourglass instability does not occur because shear deformation is evaluated by four points in an element. Displacement by SRI is close but a little smaller than that of anti-hourglass stiffness. Both SRI for an apparent soil element and for a bare soil skeleton gives the same displacement and two-point integration for soil skeleton gives smaller displacement than these cases. It may indicate that volume locking may affect displacement even when Poisson's ratio is as small as 0.3.

In the two-phase analysis, there are several element stiffness matrices related to interaction between soil skeleton and water. If two-point integration is used for matrices related to porewater ($\mathbf{K}_{uu}$, $\mathbf{K}_{uU}$, $\mathbf{K}_{UU}$), displacements are remarkably small compared with the displacement by beam theory as well as by total stress analysis. On the other hand, if SRI is used for stiffness matrix of soil skeleton with one-point integration to matrices related to porewater, result is same as that of

Table 1. Results of analysis.

Type	Method of integration	δ (m)
Beam theory		2.308×10^{-1}
Total stress	2 points	1.338×10^{-3}
	RI	Infinite
	RI + anti-hourglass stiffness	2.185×10^{-1}
	SRI	2.000×10^{-1}
	SRI (only soil skeleton)	2.000×10^{-1}
	2 points (only soil skeleton)	1.556×10^{-1}

	The number of integration point				
	K	$\mathbf{K}^{uu}$	$\mathbf{K}^{uU}$	$\mathbf{K}^{UU}$	δ (m)
u-U formulation (per one dir.)	2	2	2	2	1.338×10^{-3}
	2	2	2	1	1.779×10^{-3}
	2	2	1	2	2.654×10^{-3}
	2	2	1	1	5.219×10^{-3}
	2	1	2	2	1.779×10^{-3}
	2	1	2	1	2.654×10^{-3}
	2	1	1	2	5.219×10^{-3}
	2	1	1	1	1.556×10^{-1}
	1	2	2	2	1.350×10^{-3}
	1	2	2	1	1.800×10^{-3}
	1	2	1	2	2.700×10^{-3}
	1	2	1	1	5.400×10^{-3}
	1	1	2	2	1.800×10^{-3}
	1	1	2	1	2.700×10^{-3}
	1	1	1	2	5.400×10^{-3}
	1	1	1	1	Infinite
	SRI	1	1	1	2.000×10^{-1}

* RI : Reduced Integration.
SRI : Selective Reduced Integration.

SRI in total stress analysis; SRI gives the same element stiffness matrix both for total stress analysis and *u-U* formulation. It indicates that proposed method is appropriate and that calculation of the all matrices related to porewater is to be integrated by excess reduced integration to avoid volume locking.

Displacement by the proposed model is 22% smaller than that of total stress analysis with SRI only for soil skeleton. This indicates that element stiffness between two-point integration and SRI are different. Since there is no exact solution of this problem, it is meaningless to continue discussion on accuracy more. What important is that two displacements are of the same order as the beam theory.

It is emphasized that proposed method has an advantage in respect to the treatment than the SRI because the problem on how to treat dilatancy is not clear in the SRI method. It is also advantage of the proposed method that it shows same results as ordinary two-point integration when there is no water.

3.2 *Application in liquefaction analysis*

The 1983 Nihonkai-chubu earthquake caused significant damage in Akita Port by soil liquefaction. A typical example of damage is shown in Figure 2; sheet pile quay wall moved towards the sea and apron subsided. Liquefaction analysis is made at this site.

3.2.1 *Analyzed model*

Figure 3 shows finite element mesh. It is same as Iai and Kameoka (1993). A sheet pile wall at the quay wall and steel pipe pile for supporting pile is modeled into beam element, and a tie rod is modeled to a bar element. Dashpot is installed at the base of the model so that incident wave can be considered. It is also used along the lateral boundary and connected to free fields at both ends. Water element is build by the same method with other plane strain element, but shear modulus is set zero.

A multi spring model (Towhata and Ishihara, 1985) is used for constitutive model of soil skeleton; which

Figure 2. Damage to apron of Gaiko district, Akita port.

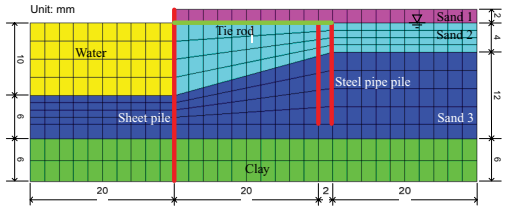

Figure 3. Finite element mesh.

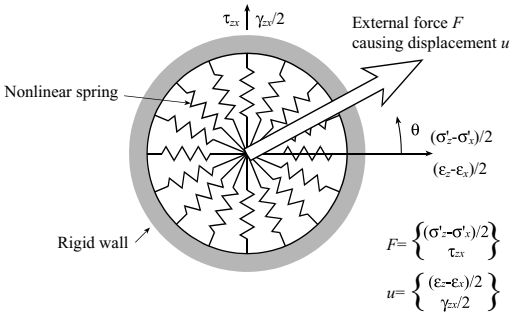

Figure 4. Schematic figure of multi-spring model.

is schematically shown in Figure 4. A hyperbolic model is employed for stress-strain model of individual spring. A generalized stress-dilatancy model (Gutierrez, 1989)

$$d\varepsilon_{vd} = \mu de^p - \frac{s_{ij} de^p_{ij}}{\sigma'_m} \tag{11}$$

is used in order to consider excess porewater generation, where ε_{vd} is volumetric strain due to dilatancy, μ is stress ratio at phase transform, e is equivalent strain, s_{ij} and e_{ij} are deviatric stress and strain, respectively, σ'_m is effective confining stress, and superscript p indicates plastic component. This type of model, however, is known to result in stable stress-strain behavior after phase transform. Therefore, we need another degrading mechanism.

At first, a degrading factor ZA is introduced such that

$$ZA = \left(1 + \left(ZA1 \sum de\right)^{ZA2}\right)^{1/ZA2-1} \tag{12}$$

and total volumetric strain due to dilatancy is expressed as

$$\varepsilon_{vd} = \sum ZF\,(d\varepsilon_{vd}) \tag{13}$$

In the same manner, stress ratio at phase transform $\sin\phi'_m$ is expressed as

$$\sin\phi'_m = \sin\phi_m + (\sin\phi^* - \sin\phi_m)(1 - ZA) \qquad (14)$$

ϕ^* is upper bound of ϕ.

A recorded earthquake motion was obtained at Akita port during the Nihonkai-chubu earthquake. Duration of the record is about 80 seconds, in which predominant part (20 seconds) shown in Figure 5 is used in the analysis as input earthquake motion. Since this wave is observed at the ground surface, it is treated as outcrop motion, and a half of it is treated as incident wave.

3.2.2 *Properties and method of analysis*

Mechanical properties of soil and other structural elements are set as shown in Tables 2 to 4, where ρ is density, n is porosity. Both G_0 and K_0 are shear and bulk modulus, respectively, and are proportional with square root of effective confining stress, and σ'_{ma} is reference strain at which G_0 and K_0 are defined. For structural element, E is Young's modulus, and A and I are cross-sectional area and moment of inertia per unit length (1 m), respectively.

Initial stress is evaluated by setting coefficient of earth pressure at rest is 0.5. In other words, initial effective overburden stress σ'_v is evaluated by $\sigma'_v = \int \rho' dh$ and horizontal normal stress is evaluated by multiplying $K_0 = 0.5$.

Numerical integration is made by Newmark's β method, where time increment is 0.01 seconds. The unbalanced force is carried into next time increment so that total equilibrium is approximately holds.

The analysis is carried out under the undrained condition, i.e., $U = u$.

3.2.3 *Result of analysis and discussion*

Displacement time history at the sheet pile and the ground is shown in Figure 6. The sheet pile wall gradually moves towards the sea, which yields about 0.3 m at the end of the analysis, which is somewhat smaller than observed displacement.

Figure 7 shows residual deformation pattern. Center part of the apron subsided, which is similar to Figure 2. However, settlement at steel pipe pile seems small, whereas it settled more in actual situation in Figure 2. If, however, steel pile was installed into the non-liquefied ground, significant settlement is not expected. It indicates that supporting ground of may

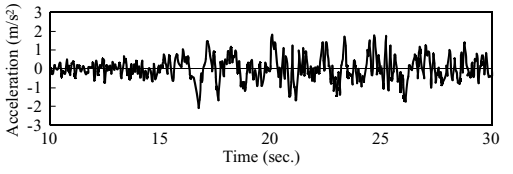

Figure 5. Predominant part of observed record at Akita port.

Table 2. Mechanical properties of soil.

Material	ρ (t/m^3)	n	G_0 (kN/m^2)	K_0 (kN/m^2)	σ'_{ma} (kN/m^2)	$\sin\phi_f$
Sand 1	1.8	0.8	33800	84500	50	0.602
Sand 2	2.0	0.8	33800	84500	50	0.602
Sand 3	2.0	0.8	72200	180500	110	0.656
Clay	1.5	0.8	74970	187430	140	0.629

Table 3. Liquefaction properties of sand.

Material	$\sin\phi_p$	ZF	G^*	$\sin\phi^*$	$ZA1$	$ZA2$
Sand 2	0.469	0.5	1000	0.6	20	2.5
Sand 3	0.469	0.1	1000	0.6	2	2.5

Table 4. Mechanical properties of structural element.

Material	ρ (t/m^3)	E (kN/m^2)	A(m)	I(m^3)
Sheer pile	7.5	2.06×10^8	0.0306	0.00086
Pipe pile	7.5	2.06×10^8	0.0058	0.000395
Tie rod	0	2.06×10^8	0.00159	0

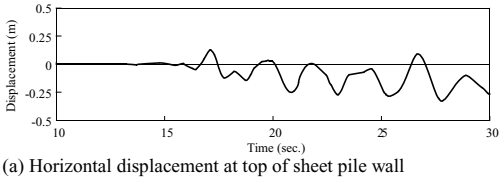

(a) Horizontal displacement at top of sheet pile wall

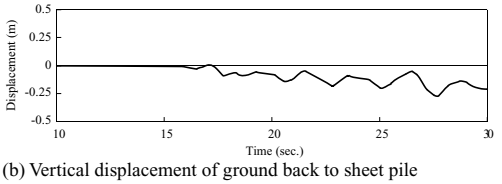

(b) Vertical displacement of ground back to sheet pile

Figure 6. Displacement time history.

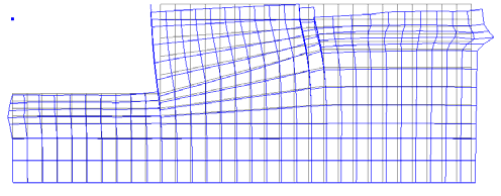

Figure 7. Residual deformation.

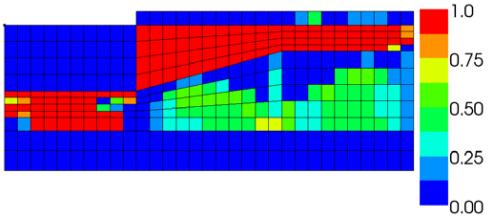

Figure 8. Residual excess porewater pressure ratio.

liquefy. However, as shown in Figure 8, supporting ground does not liquefy in the analysis.

This disagreement may explain the reason why displacement of quay wall is smaller than observed displacement. If liquefaction occurs more deep near the steel pile, rigidity in horizontal direction becomes much smaller than evaluated in this analysis. In other words, horizontal stiffness of steel pipe constrains horizontal displacement of quay wall towards the sea.

Finally, liquefaction occurs in "sand 2" in figure 3 at the back of the sheet pile quay wall, but "sand 3" does not liquefy. On the other hand, at the front of the quay wall, "sand 3" liquefies. This can be explained by considering that initial stress is smaller at the front of the quay wall than at the back of the quay wall.

In conclusion, damage of the Akita Port during the 1983 Nihonkai-chubu earthquake can be explained qualitatively, but there seems some disagreement. This may be caused that liquefaction does not occur in "sand 3" in the analysis; therefore, a more detailed consideration is required for the mechanical property of "sand 3".

4 CONCLUDING REMARKS

A new finite element formulation is proposed in the liquefaction analysis. It is based on *u-U* formulation, one of the most exact formulations of Biot's equation, and soil skeleton and water is modeled as it is. The proposed method consists of ordinary Gauss integration for integration related to soil skeleton and reduced integration for other matrices; therefore, it is more convenient to handle compared with SRI method. This method has advantage that volume locking, which occurs when Poisson's ratio comes close to 0.5, does not occur, and hourglass instability, which occurs under excess reduced integration, does not occur, too. In addition, dilatancy, which is necessary to be considered in the liquefaction analysis, can be naturally considered.

Numerical examples are carried out to evaluate accuracy of the integration scheme, and the following conclusions are obtained.

1. Volume locking as well as hourglass instability does not occur in the proposed method. Displacement is the same order as those by other methods that can avoid volume locking and hourglass instability.
2. Both total stress analysis and *u-U* formulation gives the same results when selective reduced integration is employed.
3. Displacements by two-point integration and selective reduced integration are different to each other even when Poisson's ratio is as small as 0.3.
4. It is necessary to employ reduced integration to all matrices that relate porewater in the *u-U* formulation.

Finally, analysis of Akita port that was damaged during the 1983 Nihonkai-chubu earthquake indicates that damage can be explained qualitatively, which shows ability of the proposed method. It is also recognized that modeling of soil property, especially liquefaction property, is important to obtain accurate result.

REFERENCES

Bathe, K. J. 1982. Finite element procedures in engineering analysis, Prentice-Hall, New Jersey.

Biot, M. A. 1941. General Theory of Three-dimensional Consolidation, *J. Appl Phys.* 12, pp. 155–164.

Flanagan, D. P. and Belytschko, T. 1981. A uniform strain hexahedron and quadrilateral with orthogonal hourglass control, *International Journal for Numerical Methods in Engineering* 17, pp. 679–706.

Fukutake, K. 1997. Study of three dimensional liquefaction analysis of soil-structure system considering multi-directional nature of shear deformation, *Ohsaki Research Report, No. 97-03*, Shimizu corp. (in Japanese).

Gutierrez, M. 1989. Behavior of sand during rotation of principal stress direction, *D. Eng. Thesis, University of Tokyo*.

Iai, S. and Kameoka, T. 1993. Finite element analysis of earthquake induced damage to anchored sheet pile quay walls, *Soils and Foundations*, Vol. 33, No. 1, pp. 71–91.

Japan Society of Civil Engineer. 2003. Proceeding of symposium, *Soil Liquefaction under level II Earthquake Motion*, Japan Society of Civil Engineer (in Japanese).

JGS (Japanese Geotechnical Society). 1999. *Proc. Symposium on the mechanism, prediction and design method against liquefaction* (in Japanese).

LIQCA developer team. 2002. *Material of LIQCA2D01 (2001 public version)*, p. 67 (in Japanese).

Kokusho, T. 1980. Cyclic Triaxial Test of Dynamic Soil Properties for Wide Strain Range, *Soils and Foundations* Vol. 20, No. 2, pp. 45–60.

The Japanese Geotechnical Society. 2007. Dynamic analysis of the ground, From a basic theory to the application, *Geotechnical engineering and basic theory series* 2, p. 152.

Towhata, I. and Ishihara, K. 1985. Modelling soil behavior under principal stress axes rotation, Proc. 5th International Conference for Numerical Method in Geomechanics, *Nagoya*, 1, pp. 523–530.

Yamada, T. 2007. Calculation mechanics lecture series 9, High performance finite element method, *Maruzen*, p. 152 (in Japanese).

Yasuda, S., Yoshida, N., Adachi, K., Kiku, H., Gose, S. and Masuda, T. 1990). A simplified practical method for evaluating liquefaction-induced flow, *Journal of Japan Society of Civil Engineer* 638: III(49), pp. 71–89 (in Japanese).

Yoshida, N. 1993. STADAS, A computer program for static and dynamic analysis of ground and soil-structure interaction problems, *Report, Soil Dynamics Group, The University of British Columbia, Vancouver, Canada*.

Yoshida, N. 1998. Can effective stress analysis simulates actual phenomena, Fundamental Concepts of the Design of Foundation in the Liquefiable Ground, Committee on Structural Engineering, AIJ, pp. 47–92 (in Japanese).

Yoshida, N. 1999. Basic equation of liquefaction analysis, *Proceeding of symposium announcement concerning liquefaction mechanism, forecast method, and design method*, pp. 52–59 (in Japanese).